

Influence of Postdeposition  
Annealing on the Enhanced  
Structural and Electrical Properties of  
Amorphous and Crystalline Ta<sub>2</sub>O<sub>5</sub>  
Thin Films for Dynamic Random  
Access Memory Applications

by P. C. Joshi and M. W. Cole

ARL-RP-24

June 2001

A reprint from *Journal of Applied Physics*, vol. 86, no. 2, pp. 871-880, 15 July 1999.

Approved for public release; distribution is unlimited.

20010724 081

The findings in this report are not to be construed as an official Department of the Army position unless so designated by other authorized documents.

Citation of manufacturer's or trade names does not constitute an official endorsement or approval of the use thereof.

Destroy this report when it is no longer needed. Do not return it to the originator.

# Army Research Laboratory

Aberdeen Proving Ground, MD 21005-5069

---

---

ARL-RP-24

June 2001

---

---

## Influence of Postdeposition Annealing on the Enhanced Structural and Electrical Properties of Amorphous and Crystalline Ta<sub>2</sub>O<sub>5</sub> Thin Films for Dynamic Random Access Memory Applications

P. C. Joshi and M. W. Cole

Weapons and Materials Research Directorate, ARL

A reprint from *Journal of Applied Physics*, vol. 86, no. 2, pp. 871-880, 15 July 1999.

---

---

Approved for public release; distribution is unlimited.

---

---

---

## Abstract

---

Tantalum oxide ( $\text{Ta}_2\text{O}_5$ ) thin films were fabricated on Pt-coated Si,  $n^+$ -Si, and poly-Si substrates by metalorganic solution deposition technique. The effects of postdeposition annealing on the structural, electrical, and optical properties were analyzed. The  $\text{Ta}_2\text{O}_5$  films were amorphous up to 600 °C. A well-crystallized orthorhombic phase with strong  $a$ -axis orientation was obtained at an annealing temperature of 650 °C. The refractive index was found to increase with annealing temperature and a value of 2.08 (at 630 nm) was obtained for films annealed at 750 °C. The electrical measurements were conducted on metal-insulator-metal (MIM) and metal-insulator-semiconductor capacitors. The dielectric constant of amorphous  $\text{Ta}_2\text{O}_5$  thin films was in the range 29.2–29.5 up to 600 °C, while crystalline thin films, annealed in the temperature range 650–750 °C, exhibited enhanced dielectric constant in the range 45.6–51.7. The high dielectric constant in crystalline thin films was attributed to orientation dependence of the dielectric permittivity. The dielectric loss factor did not show any appreciable dependence on the annealing temperature and was in the range 0.006–0.009. The frequency dispersion of the dielectric properties was also analyzed. The films exhibited high resistivities of the order  $10^{12}$ – $10^{15}$   $\Omega$  cm at an applied electric field of 1 MV/cm in the annealing temperature range of 500–750 °C. The measurement of current-voltage ( $I$ - $V$ ) characteristics in MIM capacitors indicated the conduction process to be bulk limited. The  $I$ - $V$  characteristics were ohmic at low fields, and Poole-Frenkel effect dominated at high fields. The temperature coefficient of capacitance was in the range 52–114 ppm/°C for films annealed in the temperature range 500–750 °C. The bias stability of capacitance, measured at an applied electric field of 1 MV/cm, was better than 1.41% for  $\text{Ta}_2\text{O}_5$  films annealed up to 750 °C. For a 0.15- $\mu\text{m}$ -thick film, a unit area capacitance of 3.0 fF/ $\mu\text{m}^2$  and a charge storage density of 22.3 fC/ $\mu\text{m}^2$  were obtained at an applied electric field of 0.5 MV/cm.

# Influence of postdeposition annealing on the enhanced structural and electrical properties of amorphous and crystalline Ta<sub>2</sub>O<sub>5</sub> thin films for dynamic random access memory applications

P. C. Joshi and M. W. Cole<sup>a)</sup>

US Army Research Laboratory, Weapons and Materials Research Directorate, Aberdeen Proving Ground, Maryland 21005

(Received 5 March 1999; accepted for publication 16 April 1999)

Tantalum oxide (Ta<sub>2</sub>O<sub>5</sub>) thin films were fabricated on Pt-coated Si, *n*<sup>+</sup>-Si, and poly-Si substrates by metalorganic solution deposition technique. The effects of postdeposition annealing on the structural, electrical, and optical properties were analyzed. The Ta<sub>2</sub>O<sub>5</sub> films were amorphous up to 600 °C. A well-crystallized orthorhombic phase with strong *a*-axis orientation was obtained at an annealing temperature of 650 °C. The refractive index was found to increase with annealing temperature and a value of 2.08 (at 630 nm) was obtained for films annealed at 750 °C. The electrical measurements were conducted on metal-insulator-metal (MIM) and metal-insulator-semiconductor capacitors. The dielectric constant of amorphous Ta<sub>2</sub>O<sub>5</sub> thin films was in the range 29.2–29.5 up to 600 °C, while crystalline thin films, annealed in the temperature range 650–750 °C, exhibited enhanced dielectric constant in the range 45.6–51.7. The high dielectric constant in crystalline thin films was attributed to orientation dependence of the dielectric permittivity. The dielectric loss factor did not show any appreciable dependence on the annealing temperature and was in the range 0.006–0.009. The frequency dispersion of the dielectric properties was also analyzed. The films exhibited high resistivities of the order of 10<sup>12</sup>–10<sup>15</sup> Ω cm at an applied electric field of 1 MV/cm in the annealing temperature range of 500–750 °C. The measurement of current-voltage (*I*-*V*) characteristics in MIM capacitors indicated the conduction process to be bulk limited. The *I*-*V* characteristics were ohmic at low fields, and Poole-Frenkel effect dominated at high fields. The temperature coefficient of capacitance was in the range 52–114 ppm/°C for films annealed in the temperature range 500–750 °C. The bias stability of capacitance, measured at an applied electric field of 1 MV/cm, was better than 1.41% for Ta<sub>2</sub>O<sub>5</sub> films annealed up to 750 °C. For a 0.15-μm-thick film, a unit area capacitance of 3.0 fF/μm<sup>2</sup> and a charge storage density of 22.3 fC/μm<sup>2</sup> were obtained at an applied electric field of 0.5 MV/cm. © 1999 American Institute of Physics. [S0021-8979(99)07914-1]

## I. INTRODUCTION

The development of future generation of dynamic random access memories (DRAMs) will require the introduction of new materials with higher dielectric constant than the conventional SiO<sub>2</sub> or silicon oxide/nitride based systems. As the supply voltages of DRAMs and available area for the capacitor decrease rapidly, the thickness of the dielectric has to be decreased considerably to maintain similar charge storage densities. However, the conventional dielectric thickness has reached a lower limit set by electron tunneling through the dielectric. The use of high dielectric constant material will make it possible to achieve similar charge storage density as conventional dielectrics at relatively larger thicknesses and lead to the design of planar or nearly planar capacitor geometry and can significantly improve yield when compared to deep trench or stack capacitor designs. Among the dielectric materials under investigation, Ta<sub>2</sub>O<sub>5</sub> is one of the most promising insulator materials for DRAM cell capacitors. Tantalum oxide thin films are attractive for scaled down capacitor in ultralarge scale integrated (ULSI) circuits because

of their high dielectric constant, low dielectric loss, low leakage current, low defect density, and good temperature and bias stability.<sup>1,2</sup> The high dielectric constant and low dielectric loss materials are also attractive for microwave applications.<sup>3</sup> Ta<sub>2</sub>O<sub>5</sub> thin films have potential for numerous microelectronic applications such as gate dielectric of metal-insulator-semiconductor (MIS) devices,<sup>4</sup> optical waveguides,<sup>5</sup> electroluminescent display devices,<sup>6</sup> and surface acoustic wave (SAW) devices.<sup>7</sup>

For successful integration into microelectronic devices, extremely reliable Ta<sub>2</sub>O<sub>5</sub> thin films are desired. Several thin film growth techniques such as anodization,<sup>8</sup> thermal oxidation,<sup>9</sup> electron-beam evaporation,<sup>10</sup> reactive sputtering,<sup>11</sup> excimer-laser assisted chemical vapor deposition,<sup>12</sup> metalorganic chemical vapor deposition (MOCVD),<sup>13</sup> ultraviolet photo chemical vapor deposition (photo-CVD),<sup>14</sup> low-pressure chemical vapor deposition (LPCVD),<sup>15</sup> and plasma-enhanced chemical vapor deposition (PECVD)<sup>16</sup> have been employed to fabricate good quality Ta<sub>2</sub>O<sub>5</sub> thin films. The properties of Ta<sub>2</sub>O<sub>5</sub> thin films have been reported to be strongly dependent on the fabrication method, nature of substrate and electrode material, and post-

<sup>a)</sup>Electronic mail: mcole.arl.mil

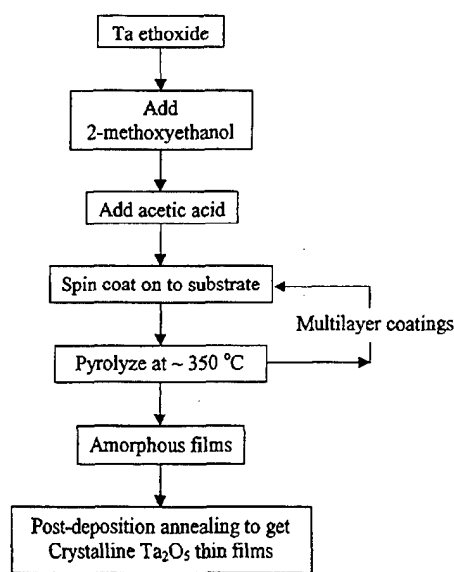


FIG. 1. Flow diagram for the MOSD processing of  $\text{Ta}_2\text{O}_5$  thin films.

deposition annealing treatment. The technical literature shows a wide variation in the reported structural, dielectric, and insulating properties of amorphous and crystalline  $\text{Ta}_2\text{O}_5$  thin films. The major focus of  $\text{Ta}_2\text{O}_5$  thin film research has been to improve the leakage current characteristics of amorphous  $\text{Ta}_2\text{O}_5$  thin films deposited on Si substrates for DRAM applications with little emphasis on structure–property correlation studies. An understanding of process–structure–property correlation is important to understand and compare various thin film studies reported in literature and exploit  $\text{Ta}_2\text{O}_5$  thin films for devices. In this article, we report on the systematic study of structural, optical, dielectric, and insulating properties of amorphous and crystalline  $\text{Ta}_2\text{O}_5$  thin films fabricated by metalorganic solution deposition (MOSD) technique which has been extensively used in thin film technology.<sup>17</sup> Detailed studies were conducted on films deposited on Pt-coated Si substrates to minimize the influence of film/substrate interface on the electrical properties and a comparison was made of the dielectric properties of films deposited on metal and semiconductor substrates to analyze the effects of film–semiconductor interface. The effects of postdeposition annealing temperature on the structural and electrical properties of  $\text{Ta}_2\text{O}_5$  thin films were also analyzed. The dominant electrical conduction mechanism in amorphous and crystalline  $\text{Ta}_2\text{O}_5$  thin films was examined through measurements of leakage current versus voltage characteristics in metal–insulator–metal (MIM) capacitors.

## II. EXPERIMENT

$\text{Ta}_2\text{O}_5$  thin films were fabricated by MOSD technique using tantalum ethoxide [ $\text{Ta}(\text{OC}_2\text{H}_5)_5$ ] as precursor. 2-methoxyethanol ( $\text{H}_3\text{COCH}_2\text{CH}_2\text{OH}$ ) was used as solvent. Figure 1 shows the general steps in the fabrication of  $\text{Ta}_2\text{O}_5$  thin films by MOSD technique. In the experiment, tantalum ethoxide was initially dissolved in 2-methoxyethanol. Finally, acetic acid ( $\text{CH}_3\text{COOH}$ ) was added to prevent rapid

hydrolysis and precipitation of the metal oxide. The viscosity and surface tension of the solution was adjusted by varying the 2-methoxyethanol content. The precursor films were coated onto various substrates by spin coating using photoresist spinner. Dust and other suspended impurities were removed from the solution by filtering through  $0.2\ \mu\text{m}$  syringe filter. The thickness of the films was controlled by adjusting the viscosity of the solution and spin speed. Pt-coated Si,  $n^+$ -Si, and poly-Si substrates were used in the study. Prior to the deposition of the films, the silicon substrates were cleaned by a room-temperature technique entitled spin etching<sup>18</sup> to remove the native silicon oxide and make the substrate surface hydrogen terminated. After spinning onto various substrates, films were kept on a hot plate (at  $\sim 350\ ^\circ\text{C}$ ) in air for 10 min to remove solvents and other organic. This step was repeated after each coating to ensure complete removal of volatile matter. The postdeposition annealing of the films was carried out in a furnace at various temperatures in an oxygen atmosphere. The structure of the films was analyzed by x-ray diffraction (XRD). The XRD patterns were recorded on a Scintag XDS 2000 diffractometer using  $\text{Cu}\ K\alpha$  radiation at 40 kV. The surface morphology of the films was examined by Digital Instrument's Dimension 3000 atomic force microscope (AFM) using tapping mode with amplitude modulation. The sample thickness and optical properties were measured by variable angle spectroscopic ellipsometry using Woollam VB-200 ellipsometer. The electrical measurements were conducted on films in MIM and MIS configurations. Several platinum electrodes were sputter deposited through a shadow mask on the top surface of the films to form MIM and MIS capacitors. Capacitance and  $\tan\ \delta$  values were measured by HP4192A LF impedance analyzer. The capacitance–voltage ( $C$ – $V$ ) characteristics were also measured with HP4192A. The insulating properties and dominant conduction mechanism in amorphous and crystalline  $\text{Ta}_2\text{O}_5$  thin films were analyzed through the measurements of leakage current versus voltage ( $I$ – $V$ ) characteristics in MIM capacitors using HP4140B semiconductor test system.

## III. RESULTS AND DISCUSSION

### A. Structure and morphology

The as-pyrolyzed films (at  $\sim 350\ ^\circ\text{C}$ ) films were amorphous in nature, and postdeposition annealing was required to impart crystallinity. The postdeposition annealing of the films was carried out in the temperature range  $500$ – $750\ ^\circ\text{C}$  in an oxygen atmosphere. Figure 2 shows the XRD patterns of the  $\text{Ta}_2\text{O}_5$  thin films deposited on Pt-coated Si substrates as a function of annealing temperature. All the films were  $0.15\ \mu\text{m}$  thick and annealed for 60 min. The absence of diffraction peaks in XRD patterns of films annealed up to  $600\ ^\circ\text{C}$  indicated that these films were amorphous. It was possible to obtain a well-crystallized phase at an annealing temperature of  $650\ ^\circ\text{C}$  with no evidence of secondary phases. As the annealing temperature was increased, the peak intensity in XRD patterns increased and the full width at half maximum (FWHM) decreased, indicating enhanced crystallinity and an increase in grain size with increasing annealing temperature.

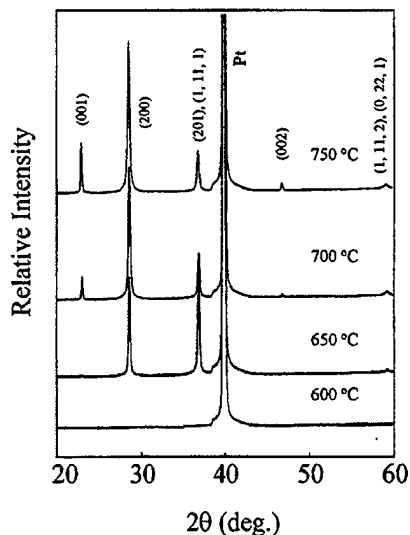


FIG. 2. X-ray diffraction patterns of Ta<sub>2</sub>O<sub>5</sub> thin films annealed at various temperatures for 60 min.

The presence of intense diffraction peak corresponding to (200) plane and the relatively weaker diffraction from (001) and (002) planes implied that the deposited Ta<sub>2</sub>O<sub>5</sub> thin films possessed a strong preferential orientation. Similar trends were observed in the XRD patterns of Ta<sub>2</sub>O<sub>5</sub> thin films deposited on silicon substrates (*n*<sup>+</sup> and poly) by the MOSD technique indicating preferential orientation. The lattice constants *a*, *b*, and *c*, calculated using (001), (200), and (1,11,1) peaks in the XRD pattern, were 6.225, 39.8521, and 3.8609 Å, respectively. These values were in good agreement with those reported for bulk Ta<sub>2</sub>O<sub>5</sub>; suggesting that that the films were crystallized in the orthorhombic phase.<sup>19</sup>

The surface morphology of Ta<sub>2</sub>O<sub>5</sub> thin films was analyzed by AFM using tapping mode with amplitude modulation. The scan area was 1 × 1 μm<sup>2</sup>. The surface morphology of the films was smooth, as shown in Fig. 3, with no cracks and defects. The films exhibited a dense microstructure and fine grain size. The average surface roughness was found to increase with increase in annealing temperature with average surface roughness value of 4 nm at 750 °C. There was no appreciable effect of the annealing temperature on the microstructure of amorphous Ta<sub>2</sub>O<sub>5</sub> thin films, while crystalline films showed an increase in grain size with increasing annealing temperature which is consistent with the XRD studies indicating an increase in peak sharpness with annealing temperature. Larger grain sizes are expected with increasing annealing temperature because of amorphous to crystalline phase transformation and increase in surface mobility, thus allowing the films to decrease its total energy by growing larger grains and decreasing its grain boundary area.

### B. Dielectric and optical properties

The dielectric properties of Ta<sub>2</sub>O<sub>5</sub> thin films were measured in terms of the dielectric constant  $\epsilon_r$  and loss tangent  $\tan \delta$ . The small signal dielectric measurements were conducted on MIM and MIS capacitors by applying an alternating current (ac) signal of 10 mV amplitude. The effects of

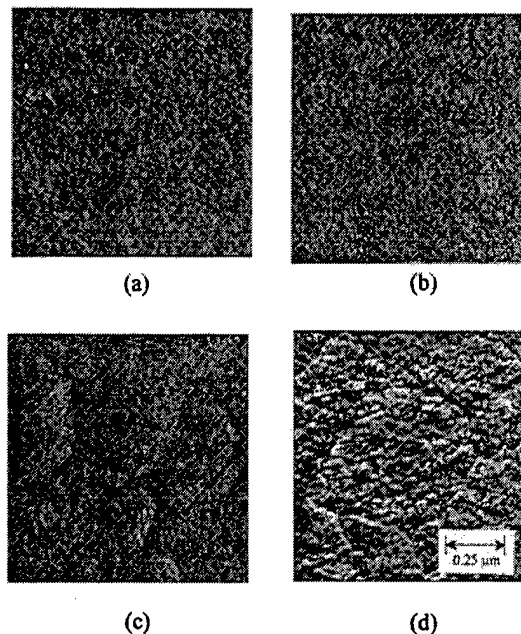


FIG. 3. AFM photographs of Ta<sub>2</sub>O<sub>5</sub> thin films annealed at (a) 500 °C, (b) 600 °C, (c) 650 °C, and (d) 750 °C.

applied frequency, film thickness, and postdeposition annealing temperature on the dielectric properties were also analyzed. Figure 4 shows the low field dielectric constant and dissipation factor of 0.15-μm-thick Ta<sub>2</sub>O<sub>5</sub> film, annealed at 750 °C, as a function of frequency. The small signal dielectric constant and dissipation factor at a frequency of 100 kHz were 51.7 and 0.008, respectively. The permittivity showed no appreciable dispersion with frequency up to about 1 MHz, as shown in Fig. 4, indicating that the values were not masked by any surface layer effects or electrode barrier effects in this frequency range. The dielectric constant was found to decrease slightly with frequency as the frequency

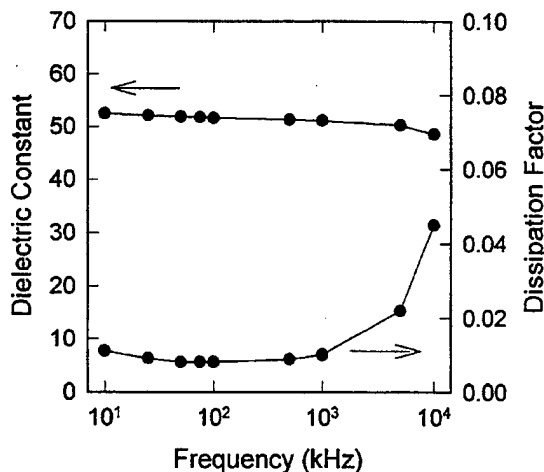


FIG. 4. Dielectric constant and dissipation factor as a function of frequency for a 0.15-μm-thick film annealed at 750 °C.

TABLE I. Effects of postdeposition annealing temperature on the dielectric and optical properties of Ta<sub>2</sub>O<sub>5</sub> thin films.

$T_A$ (°C)	$\epsilon_r$ (at 100 kHz)	$\tan \delta$	$n$ (at 630 nm)	TCK (ppm/°C)
500	29.2	0.007	1.98	+51
600	29.5	0.009	2.01	+52
650	45.6	0.009	2.05	+66
700	50.4	0.007	2.06	+77
750	51.7	0.008	2.08	+114

was increased above 1 MHz. At around the same frequency, the dissipation factor showed a rapid increase in value with frequency. For any dielectric material, the intrinsic frequency dependence of the material or the effects due to electrodes or any internal interfacial barrier may induce such a resonance. Presence of an appreciable resistance, which may be arising from intrinsic or extrinsic sources, in series with the dielectric film can affect the dielectric response at high frequencies. Similar frequency dispersion behavior due to finite resistance of the external electrodes has been reported for other dielectric materials.<sup>20</sup> In the present study, the resonance behavior was found to be extrinsic in nature as similar resonance was observed at around the same frequency for thin films of other dielectric materials having similar order of capacitance.<sup>21,22</sup> The observed resonance behavior for amorphous and crystalline Ta<sub>2</sub>O<sub>5</sub> thin films was found to be dependent on the film capacitance and shifted towards lower frequencies for larger capacitances indicating that the source of resonance was extrinsic in nature. At the frequencies of the order of a few megahertz, the stray inductance  $L$  of the contacts and wires may induce an  $L$ - $C$  resonance at a resonant frequency,  $f_r$ , given by

$$f_r = \frac{1}{2\pi\sqrt{LC}},$$

where  $C$  is the capacitance of the sample under test. For thin films having capacitance of the order of 1 nF or so, a stray inductance of the order of a few micro-Henries can induce  $L$ - $C$  resonance in the megahertz frequency range. As the resonance behavior was observed at a frequency higher than 1 MHz, all the dielectric measurements were conducted at frequencies much lower than this resonance frequency. At these frequencies, the internal accuracy of the impedance analyzer was always better than 1%.

Table I shows the effect of postdeposition annealing temperature on the dielectric properties of Ta<sub>2</sub>O<sub>5</sub> thin films. There was no appreciable effect of the annealing temperature on the dielectric properties as long as the films were in amorphous state. The dielectric constant and the dissipation factor for amorphous Ta<sub>2</sub>O<sub>5</sub> thin films were in the range 29.2–29.5 and 0.006–0.009, respectively, up to an annealing temperature of 600 °C. The dielectric constant was found to increase to 45.6 at an annealing temperature of 650 °C as the films were well crystallized. The dielectric constant of crystalline Ta<sub>2</sub>O<sub>5</sub> thin films was found to increase with increase in annealing temperature while the loss factor did not show any appreciable dependence on the annealing temperature. The

dielectric constant and the dissipation factors were in the range 45.6–51.7 and 0.006–0.009, respectively, for films annealed in the temperature range 650–750 °C. The increase in the dielectric constant of the crystalline thin films with annealing temperature may be attributed to improved crystallinity and increase in grain sizes and density of the films as indicated by XRD and AFM studies.

There is a wide variation in the reported dielectric constant of amorphous and crystalline Ta<sub>2</sub>O<sub>5</sub> thin films. The dielectric constant of amorphous and crystalline thin films has been reported in the range (14–31)<sup>11,16,23–29</sup> and (24–60),<sup>23,26,28–38</sup> respectively. The dielectric properties of thin films strongly depend on the fabrication method, nature of substrate and electrode material, postdeposition annealing treatment, crystallographic orientation, microstructure, thickness of samples, and film–substrate interface characteristics. Ta<sub>2</sub>O<sub>5</sub> exists in two modifications with a transition temperature of 1320±20 °C. The low temperature modification,  $\beta$ -Ta<sub>2</sub>O<sub>5</sub> is isostructural with the low temperature modification of Nb<sub>2</sub>O<sub>5</sub>,  $\gamma$ -Nb<sub>2</sub>O<sub>5</sub>, and it has an orthorhombic structure.<sup>39</sup> The anisotropy of the crystal structure of  $\gamma$ -Nb<sub>2</sub>O<sub>5</sub> results in a maximum of dielectric permittivity along  $a$  axis.<sup>40</sup> Thus, the dielectric constant of  $\beta$ -Ta<sub>2</sub>O<sub>5</sub> thin films is expected to show a maximum along  $a$  axis. The reported dielectric constant of crystalline Ta<sub>2</sub>O<sub>5</sub> thin films is usually higher for films showing strong  $a$ -axis orientation, while in most cases no structure–dielectric property correlation has been established to explain the observed high dielectric constant.<sup>7,38</sup> The dielectric constant of Ta<sub>2</sub>O<sub>5</sub> can be estimated using the Clausius–Mosotti equation

$$\alpha_D = \left( \frac{3V_m}{4\pi} \right) \left( \frac{\epsilon_r - 1}{\epsilon_r + 2} \right) = \alpha_{\text{ionic}} + \alpha_{\text{electronic}},$$

where  $\alpha_D$  is the dielectric polarizability,  $V_m$  is the molar volume in cubic angstroms,  $\epsilon_r$  is the real part of the complex dielectric constant,  $\alpha_{\text{ionic}}$  is the ionic polarizability, and  $\alpha_{\text{electronic}}$  is the electronic polarizability. For Ta<sub>2</sub>O<sub>5</sub> material, a dielectric constant of 45 has been calculated along  $a$ -axis using  $\alpha_D$  value of 19.72 Å<sup>3</sup> and bulk molar volume value of 88.26 Å<sup>3</sup>.<sup>19,41</sup> The Clausius–Mosotti relation shows that the dielectric permittivity strongly depends on the molar volume which in turn depends on the lattice constants. Thin films lattice constant values are strongly influenced by the nature of substrate, as one surface of the film is adhered to the substrate, as opposed to bulk material where all the surfaces are free. The lattice constant values of present thin films were found to be slightly different from those of bulk Ta<sub>2</sub>O<sub>5</sub> ( $a=6.198$ ,  $b=40.29$ , and  $c=3.888$  Å).<sup>19</sup> The slight difference in the thin film and bulk lattice constant values may be due to stress in the films since one surface of the films is attached to the substrate. The stress may also arise due to thermal expansion mismatch between the film and substrate and due to structure and growth of the films. So it is very important to compare the thin film structure, lattice constant, and morphology with bulk to establish structure–property correlation and understand the reported properties of Ta<sub>2</sub>O<sub>5</sub> thin films fabricated by various techniques. For the present Ta<sub>2</sub>O<sub>5</sub> thin films, the polarizability value was calculated using the experimentally calculated values of lattice constants

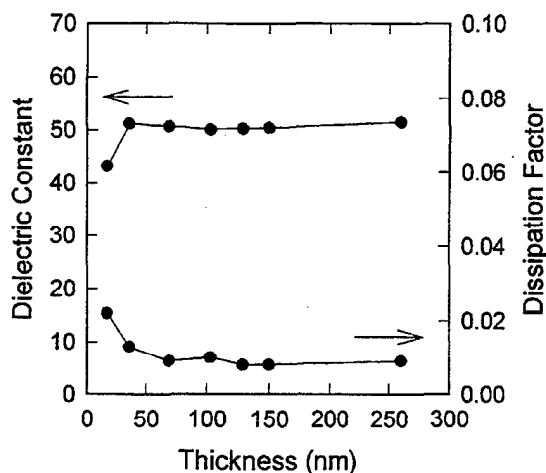


FIG. 5. Thickness dependence of dielectric constant and dissipation factor of  $\text{Ta}_2\text{O}_5$  thin films annealed at  $700^\circ\text{C}$ .

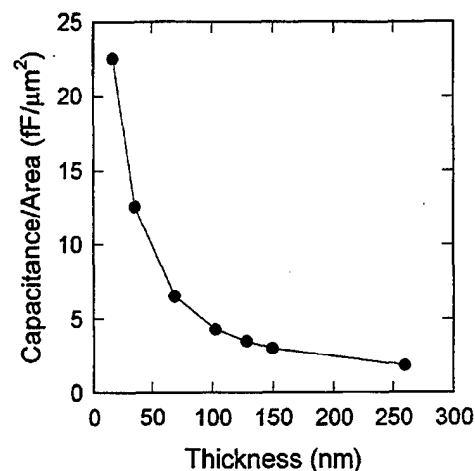


FIG. 6. Capacitance density of  $\text{Ta}_2\text{O}_5$  thin films as a function of film thickness.

and dielectric constant and a comparison was made with the value reported for bulk material. The calculated value of  $\alpha_D$ ,  $19.63 \text{ \AA}^3$ , was in good agreement with the reported value for bulk  $\text{Ta}_2\text{O}_5$  suggesting that the high dielectric constant in the present crystalline  $\text{Ta}_2\text{O}_5$  thin films was due to strong  $a$ -axis orientation which was also evident in XRD studies. This structural dependence of the dielectric properties and the wide variation in the values reported in the literature strongly emphasize the need to correlate the structural properties of thin films with their dielectric properties.

In order to analyze size effects on the dielectric properties, the dielectric measurements were conducted on  $\text{Ta}_2\text{O}_5$  thin films as a function of film thickness. Figure 5 shows the variation of low field dielectric constant and dissipation factor of  $\text{Ta}_2\text{O}_5$  thin films annealed at  $700^\circ\text{C}$  as a function of dielectric film thickness. The dielectric constant and the dissipation factor did not show any appreciable dependence on film thickness in the range 36–260 nm. At smaller thicknesses the dielectric constant was found to decrease with film thickness while the loss tangent was found to increase. The measured dielectric constant and loss factor were in the range 43.2–50.4 and 0.008–0.022, respectively, for 17–260-nm-thick films. Similar thickness dependence of the dielectric properties has been reported by others for very thin  $\text{Ta}_2\text{O}_5$  films.<sup>29,37</sup> The suggested explanations for such thickness dependence include stress in the films and the existence of barrier layer near one or both the electrodes. The stress resulting from the difference in the thermal expansion coefficient of the film and the substrate and that from the structure and growth of the films, which are usually found to have thickness dependence, may contribute to the thickness dependence of the dielectric constant. The dielectric film thickness effects on the properties are dominant in thin films when the grain size is larger than or of the order of film thickness. Under these conditions, the thickness dependence of the grain size contributes to the thickness dependence of the dielectric properties. However, the possibility of surface layer effects at lower thicknesses may not be ignored. The effect of dielectric film thickness on the charge storage ca-

capacity was also investigated. For planar capacitors, the charge storage capacity is defined by  $C_{\text{storage}} = \epsilon_0 \epsilon_r A/d$ . In conventional downscaling of physical dimensions of very large scale integrated devices, one has to reduce the area of the capacitor proportionally. Additionally, one reduces the thickness of the dielectric layer by the scaling factor, in order to achieve required capacitance density. In DRAM techniques, the attempt is to retain high  $C_{\text{storage}}$  by optimizing these capacitor parameters.  $\text{Ta}_2\text{O}_5$  can offer an order of magnitude higher capacitance density, at relatively larger thicknesses, in a DRAM cell capacitor compared to other conventional gate dielectrics such as  $\text{SiO}_2$ . Figure 6 shows the capacitance per unit area of  $\text{Ta}_2\text{O}_5$  thin films as a function of film thickness. The unit area capacitance of a 17-nm-thick film was  $22.5 \text{ fF}/\mu\text{m}^2$ . It is equivalent to a  $\text{SiO}_2$ , a conventional gate dielectric, thickness of 1.6 nm. The high charge storage capacitance per unit area of  $\text{Ta}_2\text{O}_5$  thin films even at smaller thicknesses shows their potential for high density DRAMs and integrated capacitor applications.

The effects of substrate on the dielectric properties were analyzed by measurement of dielectric properties on MIM and MIS capacitors. The MIS capacitor is the most commonly used active component for silicon ULSI circuits. The device technology has been hindered by the very high density of states at the interface of Si and insulator. A poor interface of dielectric film with silicon leads to high leakage currents, higher frequency dispersion, and high defect trapped charges. Several attempts have been made to improve the effective dielectric constant and leakage current characteristics of  $\text{Ta}_2\text{O}_5$  based MIS capacitors by optimizing the fabrication techniques and/or postdeposition annealing treatment.<sup>25,31,35,42,43</sup> In the present case, the  $\text{Ta}_2\text{O}_5$  thin films were deposited on  $n^+$ -Si and poly-Si substrates to analyze the effects of  $\text{Ta}_2\text{O}_5$  film-silicon interface on the dielectric properties. Table II shows the effect of substrate on the dielectric properties of amorphous and crystalline  $\text{Ta}_2\text{O}_5$  thin films. The dielectric properties of  $\text{Ta}_2\text{O}_5$  thin films deposited on  $n^+$ -Si and poly-Si substrates were compared with those deposited on Pt-coated Si substrates to analyze the effects of

TABLE II. Effect of substrate on the dielectric properties of Ta<sub>2</sub>O<sub>5</sub> based MIM and MIS capacitors.

Substrate	$T_{\text{Annealing}}=600\text{ }^{\circ}\text{C}$		$T_{\text{Annealing}}=750\text{ }^{\circ}\text{C}$	
	$\epsilon_r$	$\tan \delta$	$\epsilon_r$	$\tan \delta$
$n^+$ -Si	28.5	0.018	43.7	0.018
poly-Si	29.0	0.008	45.7	0.017
Pt-coated Si	29.5	0.008	51.7	0.008

silicon oxidation on effective dielectric properties. The dielectric constant of Ta<sub>2</sub>O<sub>5</sub> thin films was found to be lower on  $n^+$ -Si and poly-Si substrates, as shown in Table II, as compared to films deposited on Pt-coated Si substrates due to the growth of interfacial oxide layer on silicon substrates. There was no significant difference in the dielectric constant of amorphous Ta<sub>2</sub>O<sub>5</sub> thin films, annealed at 600 °C, deposited on various substrates indicating the absence of any appreciable oxide thickness at film-substrate interface. The films annealed at 750 °C showed much lower dielectric constant on silicon substrates as compared to films deposited on Pt-coated Si substrates indicating the presence of an appreciable oxide growth at the interface. The thickness of the oxide layer was calculated by comparing the dielectric constant of MIM and MIS capacitors by assuming the formation of a uniform oxide layer between the film and substrate with no interdiffusion. The thickness of the silicon oxide layer was calculated from the relation,  $1/C_T = 1/C_f + 1/C_{\text{SiO}_2}$ , by considering the total capacitance ( $C_T$ ) of the MIS capacitor to be a series combination of Ta<sub>2</sub>O<sub>5</sub> film capacitance ( $C_f$ ) and SiO<sub>2</sub> layer capacitance ( $C_{\text{SiO}_2}$ ). For the present Ta<sub>2</sub>O<sub>5</sub> films the thickness of the silicon oxide layer was found to be less than 2.5 nm on both  $n^+$ -Si and poly-Si substrates indicating that the combination of spin etching and MOSD technique were effective in minimizing the film-substrate interface reaction and providing good interfacial properties. Low temperature processing is essential to obtain good film/Si interfacial characteristics. Annealing temperature effects up to 1000 °C have been analyzed for Ta<sub>2</sub>O<sub>5</sub> thin films in an attempt to improve their electrical properties. Annealing at high temperatures severely degrades the film/Si interface and requires close control of processing parameters to improve the electrical properties. Low temperature processing is necessary to minimize interfacial reactions and integrate Ta<sub>2</sub>O<sub>5</sub> thin films into semiconductor devices.

The temperature and bias stability of the dielectric properties of Ta<sub>2</sub>O<sub>5</sub> thin films were also analyzed to establish their reliability for integrated electronic applications. Figure 7 shows the dielectric constant and dissipation factor of crystalline Ta<sub>2</sub>O<sub>5</sub> thin film annealed at 750 °C as a function of measurement temperature. The dielectric constant and the dissipation factor were relatively unchanged with measurement temperature in the range 25–125 °C indicating good temperature stability of the present Ta<sub>2</sub>O<sub>5</sub> thin films. The temperature coefficient of capacitance (TCK) was calculated for the present films using the equation,  $\Delta C/(C_0 \Delta T)$  where  $\Delta C$  is the change in capacitance relative to capacitance  $C_0$  at 25 °C and  $\Delta T$  is the change in temperature relative to 25 °C.

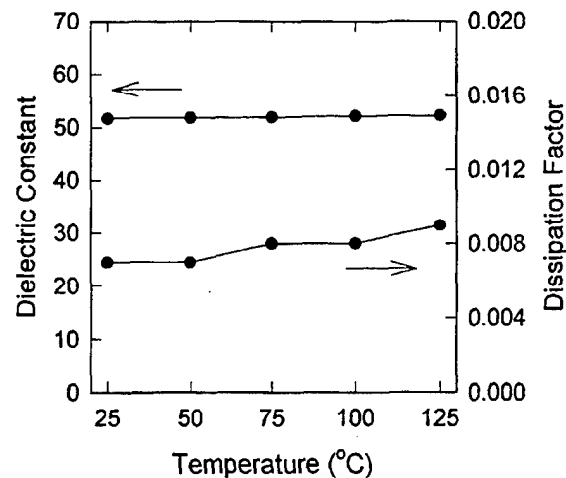
FIG. 7. Dielectric constant and dissipation factor of Ta<sub>2</sub>O<sub>5</sub> thin films as a function of measurement temperature.

Table I shows the temperature coefficient of capacitance of Ta<sub>2</sub>O<sub>5</sub> thin films, measured in the temperature range 25–125 °C, as a function of annealing temperature. The films showed a low TCK of +52 ppm/°C up to an annealing temperature of 600 °C. The TCK for the crystalline films, as shown in Table I, was found to be higher than that of amorphous films. Crystalline Ta<sub>2</sub>O<sub>5</sub> thin films annealed at 750 °C exhibited a low TCK of +114 ppm/°C establishing good reliability of present Ta<sub>2</sub>O<sub>5</sub> thin films for integrated capacitor applications. The low temperature coefficient of capacitance for the present films indicates completeness of oxidation and low defect concentration in amorphous and crystalline Ta<sub>2</sub>O<sub>5</sub> thin prepared by MOSD technique.

The optical properties of Ta<sub>2</sub>O<sub>5</sub> thin films were determined by ellipsometry. The experimentally determined psi and delta values were transformed into refractive index by assuming an optical model consisting of single homogeneous nonabsorbing film on Pt-coated Si substrates. The refractive index and the band-gap values were found to be 2.08 (at 630 nm) and 5.11 eV, respectively, for a 0.15- $\mu\text{m}$ -thick film annealed at 750 °C. The refractive index value is comparable to that reported for crystalline Ta<sub>2</sub>O<sub>5</sub> thin films prepared by MOCVD,<sup>13</sup> reactive sputtering,<sup>37</sup> and LPCVD<sup>44</sup> techniques. The effects of postdeposition annealing temperature on the refractive index were also analyzed. The refractive index value was found to increase with the increase in annealing temperature, as shown in Table I, which may be attributed to change in microstructure of the films from amorphous to crystalline, and increase in crystallinity and density of the films. There is a considerable variation in the reported refractive index of amorphous (1.70–2.18) and crystalline (1.74–2.32) Ta<sub>2</sub>O<sub>5</sub> thin films.<sup>29</sup> The refractive index of thin films strongly depends on impurities, imperfection, and voids in the films, which are incorporated during growth process. The combined effect of crystal structure, voids, imperfection, film-substrate interactions, processing conditions, etc., may be responsible for the wide variation in the reported refractive index values of Ta<sub>2</sub>O<sub>5</sub> thin films. It is difficult to com-

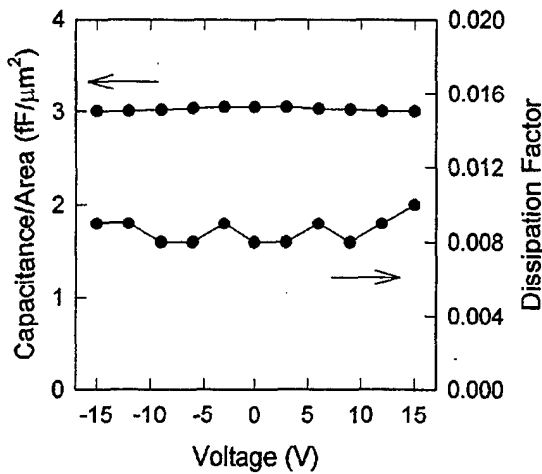


FIG. 8. *C*-*V* characteristics of Ta<sub>2</sub>O<sub>5</sub> thin films annealed at 750 °C.

pare the data of different workers unless porosity and oxygen content of the film are known.

**C. Capacitance-voltage (*C*-*V*) characteristics**

The *C*-*V* measurements were conducted on MIM capacitors to analyze the bias stability. Figure 8 shows the *C*-*V* curves of Pt/Ta<sub>2</sub>O<sub>5</sub>/Pt capacitors obtained by applying a small ac signal of 10 mV amplitude and of 100 kHz frequency across the capacitor, while the direct current (dc) electric field was swept from a negative bias to positive bias. There was no appreciable change in the capacitance of amorphous Ta<sub>2</sub>O<sub>5</sub> thin films up to an applied electric field of 1 MV/cm indicating good bias stability. It was possible to measure the change in film capacitance for crystalline thin films. The change in the film capacitance was found to be 1.41% for crystalline Ta<sub>2</sub>O<sub>5</sub> thin films, annealed at 750 °C, at an applied electric field of 1 MV/cm. The loss factor also showed good bias stability, as shown in Fig. 8, and was less than 1% up to 1 MV/cm.

A DRAM cell needs a film with high charge storage density and low leakage current density. The charge storage density, defined by  $Q_c = \epsilon_0 \epsilon_r E$ , was calculated based on the information from *C*-*V* measurements on MIM capacitors. Here, *E* is the applied electric field. Figure 9 shows the relation between the charge storage density and the applied electric field for a 0.15- $\mu$ m-thick film. The charge storage density was 22.3 fC/ $\mu$ m<sup>2</sup> at an applied electric field of 0.5 MV/cm. At this bias the leakage current density was lower than 10<sup>-8</sup> A/cm<sup>2</sup>. The high charge storage density compared to conventional dielectrics and low leakage current density suggest the suitability of present Ta<sub>2</sub>O<sub>5</sub> thin films for integrated capacitor applications.

**D. Leakage current characteristics**

Leakage current is one of the limiting factors for the suitability of a dielectric material for DRAM applications. In a DRAM cell, the stored charge on a capacitor leaks off with time through various leakage mechanisms, and a periodic refreshing is required to maintain the charge above a thresh-

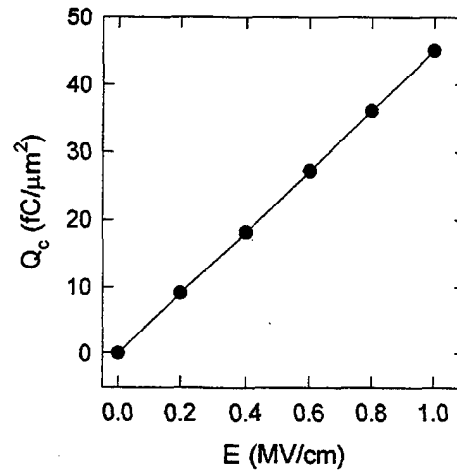


FIG. 9. Charge storage density of Ta<sub>2</sub>O<sub>5</sub> thin films as a function of applied electric field.

old for reliable operation. Thus, the leakage current characteristics of the storage capacitor dielectric are very important in a DRAM cell. The leakage current characteristics of Ta<sub>2</sub>O<sub>5</sub> thin films were measured using MIM capacitors by applying dc voltages with a step delay time of 30 s. A delay of 30 s after applying the voltage gave current readings close to the ones measured after much longer waiting times. Figure 10 shows the leakage current density versus electric field characteristics of 0.15- $\mu$ m-thick films as a function of annealing temperature. The leakage current density showed a strong dependence on the postdeposition annealing temperature and was considerably higher for crystalline thin films as compared to amorphous thin films. The resistivity of amorphous thin films was found to be of the order of 10<sup>15</sup>  $\Omega$  cm, as shown in Table III, while that of crystalline thin films was of the order of 10<sup>12</sup>  $\Omega$  cm at an applied electric field of 1 MV/cm. The high resistivity observed in the present films

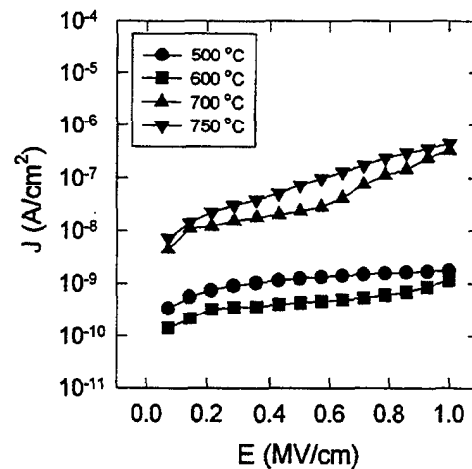


FIG. 10. *J*-*E* characteristics of Ta<sub>2</sub>O<sub>5</sub> thin films annealed in the temperature range 500-750 °C.

TABLE III. Effect of postdeposition annealing temperature on the resistivity, high frequency dielectric permittivity  $\epsilon_\infty$ , and parameter  $\alpha$  of 0.15- $\mu\text{m}$ -thick Pt/Ta<sub>2</sub>O<sub>5</sub>/Pt capacitors.

$T_A$ (°C)	Resistivity ( $\Omega\text{ cm}$ ) (at 1 MV/cm)	$\epsilon_{\infty, \text{optical}}$	$\alpha$ ( $\epsilon_{\infty, \text{electrical}} = \epsilon_{\infty, \text{optical}}$ )
500	$6 \times 10^{14}$	3.92	1.20
600	$9 \times 10^{14}$	4.04	1.22
700	$3 \times 10^{12}$	4.24	2.00
750	$2 \times 10^{12}$	4.33	2.00

shows the completeness of phase formation and oxidation of Ta<sub>2</sub>O<sub>5</sub> thin films prepared by MOSD technique. In the amorphous phase the leakage current density was found to decrease with the increase in temperature, while crystalline thin films showed an increase in leakage current with annealing temperature. Several reports exist in literature showing an increase in leakage current density of Ta<sub>2</sub>O<sub>5</sub> thin films as a result of crystallization.<sup>10,23,25,28</sup> Most of these reports focus on the properties of Ta<sub>2</sub>O<sub>5</sub> thin films deposited on Si substrates. The increase in leakage current density has been attributed to various factors such as oxygen vacancy, impurity (carbon/hydrocarbon) content, presence of incompletely oxidized silicon at the grain boundaries near film/substrate interface. In this study the leakage current characteristics of Ta<sub>2</sub>O<sub>5</sub> thin films were analyzed in MIM configuration, so no interfacial effects were expected in the annealing temperature range of 500–750 °C to contribute to the observed leakage current behavior. The leakage current of thin film strongly depends on the various material related parameters such as composition, structure, impurities, homogeneity, stress, and local effects (compositional variations, dopant segregation, grain boundaries, pores, high defect density, etc.). The structural imperfections and stress strongly influence the electrical properties of amorphous thin films. The decrease in the leakage current density of amorphous Ta<sub>2</sub>O<sub>5</sub> thin films can be attributed to the decrease in defect density, compressive stress, and increase in oxidation with increasing annealing temperature. The coordination number of oxygen atoms to Ta atoms has been reported to increase with increase in annealing temperature for LPCVD deposited Ta<sub>2</sub>O<sub>5</sub> thin films.<sup>25</sup> The reduction in stress and defect density, which are found to be annealing temperature dependent, will lead to an improvement in leakage current characteristics. The compressive stress of dc magnetron sputtered Ta<sub>2</sub>O<sub>5</sub> thin films was found to decrease with increase in annealing temperature which is due to decrease in amount of disorder.<sup>45</sup> The higher annealing temperatures are also expected to decrease the defect density in amorphous thin films. So the observed improvement in the leakage current of amorphous Ta<sub>2</sub>O<sub>5</sub> thin films with increasing annealing temperature may be attributed to decrease in film stress and defect density, and improved oxidation. The crystalline thin film exhibited much higher leakage current than the amorphous thin films. This can be explained in terms of the formation of grain boundaries in crystalline thin films as observed in AFM studies. These grain boundaries serve as a new leakage current path, resulting in poor leakage current characteristics. At high fields, the grain boundary conduction may be larger than the

grain conductivity setting large tunneling currents through these grain boundary layers. Even though the film density was found to increase with increase in annealing temperature, as observed by optical studies, the leakage current density can increase due to introduction of a number of defects, especially at the grain boundaries, due to large internal stress resulting from the phase transformation.

The steady state field dependent dc conductivity was examined by the measurement of  $I$ - $V$  characteristics in MIM capacitors. Several electrical processes allow electrical charges to move in insulators, leading to sizeable current densities, especially when the insulating film is thin (typically less than 1  $\mu\text{m}$ ). For thin insulating films of the order of 1  $\mu\text{m}$ , if an appreciable voltage can be sustained (of the order of few volts), the field strength is of the order of  $10^5$  V/cm and greater. The low field properties are usually ohmic in nature, that is, current  $I$  is linear with voltage  $V$ . At high fields these films exhibit nonlinear  $I$ - $V$  relationship. Generally, the high field characteristics cannot be adequately described by a single conduction process; usually the different field strength ranges manifest different electrical phenomena. An understanding of the mechanisms of nonlinear conductivity in thin insulators is pertinent to the development of thin film devices for microelectronics. In general, the leakage current in an insulator is either controlled by the film-electrode interface or bulk of the insulator. The  $I$ - $V$  characteristics of the present Ta<sub>2</sub>O<sub>5</sub> thin films were found to be ohmic at low fields and highly nonlinear, as shown in Fig. 10, at high fields. The leakage current characteristics showed thickness dependence even at low applied voltages indicating bulk limited current conduction.<sup>46</sup> There was no change in the magnitude of conductivity with change in the polarity of the applied voltage, which also indicated the conduction process to be bulk limited and not electrode limited. These films exhibited high resistivities in the range  $10^{12}$ – $10^{15}$   $\Omega\text{ cm}$ . In this range of resistivities, the possible dominant conduction mechanisms may be (a) tunneling, (b) Poole-Frenkel effect, and/or (c) space-charge-limited conduction. As the thickness of the films was well above 50 nm, the tunneling process was ruled out. Poole-Frenkel effect is the flow of trapped charge carriers in insulator through lowering of potential barrier in the bulk of the insulator due to applied electric field. The barrier arises due to the Coulombic potentials surrounding ionized sites in the film. The electrons having enough energy to transit over the energy barrier contribute to the current. The current density-electric field ( $J$ - $E$ ) relation for Poole-Frenkel flow is given by the equation<sup>47</sup>

$$J = AE \exp\left(-\frac{q\phi_0}{k_B T}\right) \exp\left(\frac{\beta_{\text{PF}}}{\alpha k_B T} E^{1/2}\right),$$

with

$$\beta_{\text{PF}} = \left(\frac{q^3}{\pi \epsilon_0 \epsilon_\infty}\right)^{1/2},$$

where  $A$  is a constant,  $\phi_0$  is the metal-insulator barrier height,  $k_B$  is the Boltzmann constant,  $T$  is the absolute temperature,  $\alpha$  is a parameter,  $1 \leq \alpha \leq 2$ , which takes into account the trapping sites in insulator,  $\beta_{\text{PF}}$  is the Poole-Frenkel constant,  $q$  is the electronic charge,  $\epsilon_0$  is the permittivity of free

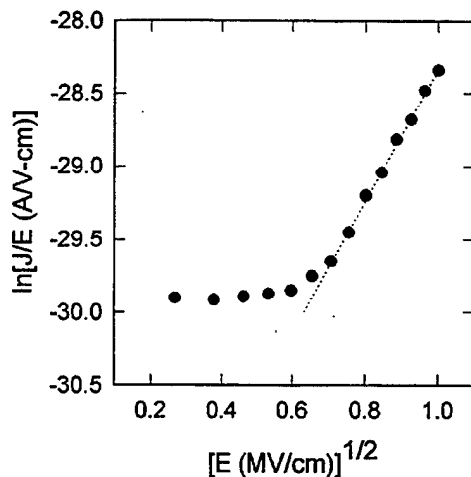


FIG. 11.  $J$ - $E$  characteristics plotted as  $\ln(J/E)$  vs  $E^{1/2}$ . The linearity at high fields indicates the presence of Poole-Frenkel effect.

space, and  $\epsilon_\infty$  is the high frequency dielectric constant. The parameter  $\alpha$  is equal to 1 for a trap free insulator, while the value is between 1 and 2, indicating a trap-modulated conduction process, depending on the location of the Fermi level. Figure 11 shows the  $\ln(J/E)$  versus  $E^{1/2}$  plot for  $\text{Ta}_2\text{O}_5$  thin film. The straight line behavior of this plot at high fields indicated the Poole-Frenkel flow to be the dominant conduction mechanism. Similar straight line behavior was observed in the high field regime of  $\ln(J/E)$  versus  $E^{1/2}$  plots for both amorphous and crystalline thin films annealed in the temperature range 500–750 °C indicating that the nonohmic conduction in  $\text{Ta}_2\text{O}_5$  thin films was due to Poole-Frenkel flow. However, the onset of this high field regime was found to be shifted to lower fields, from 1.4 to 0.6 MV/cm, with increase in annealing temperature from 500 to 700 °C. The slope of the straight line region in  $\ln(J/E)$  versus  $E^{1/2}$  plots at high fields is given by the expression

$$\text{slope} = \frac{d \ln(J/E)}{dE^{1/2}} = \frac{\beta_{\text{PF}}}{\alpha k_B T}$$

The value of the coefficient  $\beta_{\text{PF}}$  was calculated from the slope of the straight line region. The high frequency dielectric constant  $\epsilon_\infty$  was determined from the calculated values of  $\beta_{\text{PF}}$  for both amorphous and crystalline thin films. The high frequency dielectric constant value obtained from  $J$ - $E$  characteristics was compared to that calculated using the refractive index value,  $\epsilon_\infty = n^2$ , determined from ellipsometry studies to establish the dominant conduction mechanism in present  $\text{Ta}_2\text{O}_5$  thin films. The value of  $\epsilon_\infty$  calculated from the slope of  $\ln(J/E)$  versus  $E^{1/2}$  plot,  $\epsilon_\infty = 4.48$ , was in good agreement, for  $\alpha = 2$ , to that calculated using the refractive index value,  $\epsilon_\infty = n^2 = 4.33$ , for  $\text{Ta}_2\text{O}_5$  thin film annealed at 750 °C verifying Poole-Frenkel flow to be the dominant conduction mechanism in the present films. For crystalline thin films the high frequency dielectric  $\epsilon_\infty$  constant obtained from  $J$ - $E$  characteristics was in good agreement, as shown in Table III, to that obtained from optical data for  $\alpha = 2$ . However, for amorphous thin films the value of parameter  $\alpha$

was found to be less than 2 for a good agreement between  $\epsilon_\infty$  values obtained from electrical and optical studies indicating that the trap concentration was lower in amorphous thin films as compared to crystalline thin films.

#### IV. CONCLUSIONS

$\text{Ta}_2\text{O}_5$  thin films exhibiting good structural, dielectric, and insulating properties were successfully deposited on Pt-coated Si,  $n^+$ -Si, and poly-Si substrates by MOSD technique. The effects of postdeposition annealing temperature on the structural, optical, and electrical properties of amorphous and crystalline  $\text{Ta}_2\text{O}_5$  thin films were investigated. The films were amorphous up to 600 °C, and a crystalline orthorhombic phase with strong  $a$ -axis orientation was obtained at 650 °C. The surface morphology of the films was smooth with no cracks and defects while the grain size was found to increase with the increase in annealing temperature. The dielectric constant of amorphous thin films, annealed up to 600 °C, was in the range 29.2–29.5 which matches well with the commonly reported value. However, crystalline thin films exhibited significantly enhanced dielectric constant in the range 45.6–51.7 for films annealed in the temperature range 650–750 °C. The comparison of theoretical and experimentally calculated values of dielectric constant establish the orientation dependence of dielectric permittivity to be the main reason for the observed high dielectric constant in present  $\text{Ta}_2\text{O}_5$  thin films. The loss factor did not show any appreciable dependence on the annealing temperature and was in the range 0.006–0.009 for films annealed in the temperature range 500–750 °C. The films deposited on  $n^+$ -Si and poly-Si substrates exhibited good film/silicon interfacial characteristics. The growth of the oxide layer at the interface was calculated to be lower than 2.5 nm at an annealing temperature of 750 °C indicating that the combination of spin etching and MOSD technique was effective in minimizing the film-substrate interface reaction and providing good interfacial characteristics. The electrical properties of amorphous and crystalline  $\text{Ta}_2\text{O}_5$  thin films were strongly influenced by the annealing temperature. The resistivity of amorphous thin films was found to increase with annealing temperature, while that of crystalline thin films was found to decrease. The decrease in leakage current of amorphous  $\text{Ta}_2\text{O}_5$  thin films with increasing annealing temperature was attributed to the completeness of oxidation, and decrease in stress and defect density. The increase in leakage current density of crystalline thin films with annealing temperature was due to grain boundary contribution as the grain size was found to increase with annealing temperature and crystal induced defects as a result of stress arising due to phase transformation.  $\text{Ta}_2\text{O}_5$  thin films exhibited high resistivity, measured at an applied electric field of 1 MV/cm, in the range  $10^{12}$ – $10^{15}$   $\Omega$  cm for amorphous and crystalline thin films. The  $I$ - $V$  characteristics were found to be ohmic at low fields and Poole-Frenkel effect was dominant at high fields. The value of the parameter  $\alpha$  was found to increase with increase in annealing temperature indicating an increase in trap concentration with annealing temperature. The films exhibited good temperature and bias stability of dielectric properties.

The temperature coefficient of capacitance was in the range 52–114 ppm/°C for films annealed in the temperature range 500–750 °C. It was not possible to measure any appreciable change in the capacitance of amorphous films up to an applied electric field of 1 MV/cm indicating completeness of oxidation and low defect concentration. The bias stability of capacitance was 1.41% at an applied electric field of 1 MV/cm. The high resistivity, low temperature coefficient of capacitance, and good bias stability of dielectric properties establish the reliability of Ta<sub>2</sub>O<sub>5</sub> thin films for microelectronic applications. For a 0.15- $\mu$ m-thick film, a unit area capacitance of 3.0 fF/ $\mu$ m<sup>2</sup> and a charge storage density of 22.3 fC/ $\mu$ m<sup>2</sup> were obtained at an applied electric field of 0.5 MV/cm. The high dielectric constant, low dielectric loss, low leakage current density, and good temperature and bias stability suggest the suitability of Ta<sub>2</sub>O<sub>5</sub> thin films as capacitor dielectric layer for DRAMs and integrated electronic applications.

- <sup>1</sup>M. Anthony, S. Summerfelt, and C. Teng, *Texas Instr. Tech. J.* **12**, 30 (1995).
- <sup>2</sup>P. Balk, *Adv. Mater.* **7**, 703 (1995).
- <sup>3</sup>F. S. Barnes, J. Price, A. Hermann, Z. Zhang, H.-D. Wu, D. Galt, and A. Naziripour, *Integr. Ferroelectr.* **8**, 171 (1995).
- <sup>4</sup>M. Matsui, H. Nagayoshi, G. Muto, S. Tanimoto, K. Kuroiwa, and Y. Tarui, *Jpn. J. Appl. Phys., Part 1* **29**, 62 (1990).
- <sup>5</sup>H. Terui and M. Kobayashi, *Appl. Phys. Lett.* **32**, 666 (1978).
- <sup>6</sup>J. Mita, M. Koizumi, H. Kanno, T. Hayashi, Y. Sekido, and K. Nihei, *Jpn. J. Appl. Phys., Part 2* **26**, L541 (1987).
- <sup>7</sup>Y. Nakagawa and T. Okada, *J. Appl. Phys.* **68**, 556 (1990).
- <sup>8</sup>M. A. Mohammed and D. V. Morgan, *Thin Solid Films* **176**, 45 (1989).
- <sup>9</sup>D. J. Smith and L. Young, *IEEE Trans. Electron Devices* **ED-28**, 22 (1981).
- <sup>10</sup>G. S. Oehrlein, F. M. d'Heurle, and A. Reisman, *J. Appl. Phys.* **55**, 3715 (1984).
- <sup>11</sup>A. Pignolet, G. M. Rao, and S. B. Krupanidhi, *Thin Solid Films* **258**, 230 (1995).
- <sup>12</sup>J. Zhang, L. Bie, V. Dusastre, and I. W. Boyd, *Thin Solid Films* **318**, 252 (1998).
- <sup>13</sup>C. H. An and K. Sugimoto, *J. Electrochem. Soc.* **141**, 853 (1994).
- <sup>14</sup>S. Tanimoto, M. Matsui, K. Kamisako, K. Kuroiwa, and Y. Tarui, *J. Electrochem. Soc.* **139**, 320 (1992).
- <sup>15</sup>S. C. Sun and T. F. Chen, *Tech. Dig. Int. Electron Devices Meet.* **1996**, 687.
- <sup>16</sup>F. C. Chiu, J. J. Wang, J. Y. Lee, and S. C. Wu, *J. Appl. Phys.* **81**, 6911 (1997).
- <sup>17</sup>L. C. Klein, *Sol-Gel Technology for Thin Film, Fibers, Preforms, Electronics and Specialty Shapes* (Noyes, Park Ridge, NJ, 1988).
- <sup>18</sup>D. B. Fenner, D. K. Biegelsen, and R. D. Bringans, *J. Appl. Phys.* **66**, 419 (1989).
- <sup>19</sup>R. S. Roth, J. L. Waring, and H. S. Parker, *J. Solid State Chem.* **2**, 445 (1970).
- <sup>20</sup>M. Sayer, A. Mansingh, A. K. Arora, and A. Lo, *Integr. Ferroelectr.* **1**, 129 (1992).
- <sup>21</sup>P. C. Joshi and S. B. Desu, *Appl. Phys. Lett.* **73**, 1080 (1998).
- <sup>22</sup>P. C. Joshi and S. B. Desu, *J. Appl. Phys.* **80**, 2349 (1996).
- <sup>23</sup>J. V. Grahn, P. E. Hellberg, and E. Olsson, *J. Appl. Phys.* **84**, 1632 (1998).
- <sup>24</sup>V. Mikhaelashvili, Y. Betzer, I. Prudnikov, M. Orenstein, D. Ritter, and G. Eisenstein, *J. Appl. Phys.* **84**, 6747 (1998).
- <sup>25</sup>B. K. Moon, C. Isobe, and J. Aoyama, *J. Appl. Phys.* **85**, 1731 (1999).
- <sup>26</sup>C. Chaneliere, S. Four, J. L. Autran, R. A. B. Devine, and N. P. Sandler, *J. Appl. Phys.* **83**, 4823 (1998).
- <sup>27</sup>W. D. Westwood, R. J. Boynton, and S. J. Ingrej, *J. Vac. Sci. Technol.* **11**, 381 (1974).
- <sup>28</sup>S. Ezhilvalavan and T. Y. Tseng, *J. Appl. Phys.* **83**, 4797 (1998).
- <sup>29</sup>H. Treichel, A. Mitwalski, G. Tempel, G. Zorn, W. Kern, N. Sandler, and A. P. Lane, *Mater. Res. Soc. Symp. Proc.* **282**, 557 (1993).
- <sup>30</sup>N. Rausch and E. P. Bulte, *Microelectron. J.* **25**, 533 (1994).
- <sup>31</sup>I. Kim, J. S. Kim, O. S. Kwon, S. T. Ahn, J. S. Chun, and W. J. Lee, *J. Electron. Mater.* **24**, 1435 (1995).
- <sup>32</sup>W. S. Lau, P. W. Qian, N. P. Sandler, K. A. McKinley, and P. K. Chu, *Jpn. J. Appl. Phys., Part 1* **36**, 661 (1997).
- <sup>33</sup>W. R. Hitchens, W. C. Krusell, and D. M. Dobkin, *J. Electrochem. Soc.* **140**, 2615 (1993).
- <sup>34</sup>W. H. Knausenberger and R. N. Tauber, *J. Electrochem. Soc.* **120**, 927 (1973).
- <sup>35</sup>T. Aoyama, S. Saida, Y. Okayama, M. Fujisaki, K. Imai, and T. Arikado, *J. Electrochem. Soc.* **143**, 977 (1996).
- <sup>36</sup>P. A. Murawala, M. Sawai, T. Tatsuta, O. Tsuji, S. Fujita, and S. Fujita, *Jpn. J. Appl. Phys., Part 1* **32**, 368 (1993).
- <sup>37</sup>S. Roberts, J. Ryan, and L. Nesbit, *J. Electrochem. Soc.* **133**, 1405 (1986).
- <sup>38</sup>W. B. Westphal and A. Sils, *US National Technical Information Service AFML-TR-72-39* (1972), p. 243.
- <sup>39</sup>P. Kofstad, *Nonstoichiometry, Diffusion, and Electrical Conductivity in Binary Metal Oxides* (R. E. Krieger, Florida, 1983).
- <sup>40</sup>F. P. Emmenegger and M. L. A. Robinson, *J. Phys. Chem. Solids* **29**, 1673 (1968).
- <sup>41</sup>R. D. Shannon, *J. Appl. Phys.* **73**, 348 (1993).
- <sup>42</sup>S. Kamiyama, P. Y. Lesaichere, H. Suzuki, A. Sakai, I. Nishiyama, and A. Ishitani, *J. Electrochem. Soc.* **140**, 1617 (1993).
- <sup>43</sup>H. Shinriki and M. Nakata, *IEEE Trans. Electron Devices* **38**, 455 (1991).
- <sup>44</sup>N. Rausch and E. P. Bulte, *Microelectron. J.* **24**, 421 (1993).
- <sup>45</sup>S. W. Park and H. B. Im, *Thin Solid Films* **207**, 258 (1992).
- <sup>46</sup>M. Stuart, *Phys. Status Solidi* **23**, 595 (1967).
- <sup>47</sup>J. G. Simmons, in *Handbook of Thin Film Technology*, edited by L. I. Maissel and R. Glang (McGraw-Hill, New York, 1970), Ch. 14.

<u>NO. OF COPIES</u>	<u>ORGANIZATION</u>
2	DEFENSE TECHNICAL INFORMATION CENTER DTIC OCA 8725 JOHN J KINGMAN RD STE 0944 FT BELVOIR VA 22060-6218
1	HQDA DAMO FDT 400 ARMY PENTAGON WASHINGTON DC 20310-0460
1	OSD OUSD(A&T)/ODDR&E(R) DR R J TREW 3800 DEFENSE PENTAGON WASHINGTON DC 20301-3800
1	COMMANDING GENERAL US ARMY MATERIEL CMD AMCRDA TF 5001 EISENHOWER AVE ALEXANDRIA VA 22333-0001
1	INST FOR ADVNCD TCHNLGY THE UNIV OF TEXAS AT AUSTIN 3925 W BRAKER LN STE 400 AUSTIN TX 78759-5316
1	DARPA SPECIAL PROJECTS OFFICE J CARLINI 3701 N FAIRFAX DR ARLINGTON VA 22203-1714
1	US MILITARY ACADEMY MATH SCI CTR EXCELLENCE MADN MATH MAJ HUBER THAYER HALL WEST POINT NY 10996-1786
1	DIRECTOR US ARMY RESEARCH LAB AMSRL D DR D SMITH 2800 POWDER MILL RD ADELPHI MD 20783-1197

<u>NO. OF COPIES</u>	<u>ORGANIZATION</u>
1	DIRECTOR US ARMY RESEARCH LAB AMSRL CI AI R 2800 POWDER MILL RD ADELPHI MD 20783-1197
3	DIRECTOR US ARMY RESEARCH LAB AMSRL CI LL 2800 POWDER MILL RD ADELPHI MD 20783-1197
3	DIRECTOR US ARMY RESEARCH LAB AMSRL CI IS T 2800 POWDER MILL RD ADELPHI MD 20783-1197
	<u>ABERDEEN PROVING GROUND</u>
2	DIR USARL AMSRL CI LP (BLDG 305)

NO. OF  
COPIES ORGANIZATION

- 1 ARL ALC  
CHIEF ARL SEDD  
RF ELECTRONICS DIV  
B WALLACE  
2800 POWDER MILL RD  
ADELPHI MD 20783
- 1 ARL SEDD  
CHIEF SEDD ARL  
RF ELECTRONICS DIV  
T OLDHAM  
2800 POWDER MILL RD  
ADELPHI MD 20783
- 1 ARL SEDD  
BRANCH CHIEF  
RF ELECTRONICS DIV  
M PATTERSON  
2800 POWDER MILL RD  
ADELPHI MD 20783
- 1 ARL SEDD  
RF ELECTRONICS DIV  
B GIEL  
2800 POWDER MILL RD  
ADELPHI MD 20783
- 1 ARL SEDD  
RF ELECTRONICS DIV  
M DUBEY  
2800 POWDER MILL RD  
ADELPHI MD 20783
- 1 ARL SEDD  
RF ELECTRONICS DIV  
K JONES  
2800 POWDER MILL RD  
ADELPHI MD 20783

# REPORT DOCUMENTATION PAGE

Form Approved  
OMB No. 0704-0188

Public reporting burden for this collection of information is estimated to average 1 hour per response, including the time for reviewing instructions, searching existing data sources, gathering and maintaining the data needed, and completing and reviewing the collection of information. Send comments regarding this burden estimate or any other aspect of this collection of information, including suggestions for reducing this burden, to Washington Headquarters Services, Directorate for Information Operations and Reports, 1215 Jefferson Davis Highway, Suite 1204, Arlington, VA 22202-4302, and to the Office of Management and Budget, Paperwork Reduction Project (0704-0188), Washington, DC 20503.

1. AGENCY USE ONLY (Leave blank)		2. REPORT DATE June 2001	3. REPORT TYPE AND DATES COVERED Reprint, August 1998—February 1999	
4. TITLE AND SUBTITLE Influence of Postdeposition Annealing on the Enhanced Structural and Electrical Properties of Amorphous and Crystalline Ta <sub>2</sub> O <sub>5</sub> Thin Films for Dynamic Random Access Memory Applications			5. FUNDING NUMBERS 18M431	
6. AUTHOR(S) P. C. Joshi and M. W. Cole				
7. PERFORMING ORGANIZATION NAME(S) AND ADDRESS(ES) U.S. Army Research Laboratory ATTN: AMSRL-WM-MC Aberdeen Proving Ground, MD 21005-5069			8. PERFORMING ORGANIZATION REPORT NUMBER ARL-RP-24	
9. SPONSORING/MONITORING AGENCY NAMES(S) AND ADDRESS(ES)			10. SPONSORING/MONITORING AGENCY REPORT NUMBER	
11. SUPPLEMENTARY NOTES				
12a. DISTRIBUTION/AVAILABILITY STATEMENT Approved for public release; distribution is unlimited.			12b. DISTRIBUTION CODE	
13. ABSTRACT (Maximum 200 words) Tantalum oxide (Ta <sub>2</sub> O <sub>5</sub> ) thin films were fabricated on Pt-coated Si, n + -Si, and poly-Si substrates by metalorganic solution deposition technique. The effects of postdeposition annealing on the structural, electrical, and optical properties were analyzed. The Ta <sub>2</sub> O <sub>5</sub> films were amorphous up to 600 °C. A well-crystallized orthorhombic phase with strong a-axis orientation was obtained at an annealing temperature of 650 °C. The refractive index was found to increase with annealing temperature and a value of 2.08 (at 630 nm) was obtained for films annealed at 750 °C. The electrical measurements were conducted on metal-insulator-metal (MIM) and metal-insulator-semiconductor capacitors. The dielectric constant of amorphous Ta <sub>2</sub> O <sub>5</sub> thin films was in the range 29.2–29.5 up to 600 °C, while crystalline thin films, annealed in the temperature range 650–750 °C, exhibited enhanced dielectric constant in the range 45.6–51.7. The high dielectric constant in crystalline thin films was attributed to orientation dependence of the dielectric permittivity. The dielectric loss factor did not show any appreciable dependence on the annealing temperature and was in the range 0.006–0.009. The frequency dispersion of the dielectric properties was also analyzed. The films exhibited high resistivities of the order 10 <sup>12</sup> –10 <sup>15</sup> Ω cm at an applied electric field of 1 MV/cm in the annealing temperature range of 500–750 °C. The measurement of current-voltage (I-V) characteristics in MIM capacitors indicated the conduction process to be bulk limited. The I-V characteristics were ohmic at low fields, and Poole-Frenkel effect dominated at high fields. The temperature coefficient of capacitance was in the range 52–114 ppm/°C for films annealed in the temperature range 500–750 °C. The bias stability of capacitance, measured at an applied electric field of 1 MV/cm, was better than 1.41% for Ta <sub>2</sub> O <sub>5</sub> films annealed up to 750 °C. For a 0.15-μm-thick film, a unit area capacitance of 3.0 fF/μm <sup>2</sup> and a charge storage density of 22.3 fC/μm <sup>2</sup> were obtained at an applied electric field of 0.5 MV/cm.				
14. SUBJECT TERMS DRAM, microwave devices, dielectric materials			15. NUMBER OF PAGES 15	
			16. PRICE CODE	
17. SECURITY CLASSIFICATION OF REPORT UNCLASSIFIED	18. SECURITY CLASSIFICATION OF THIS PAGE UNCLASSIFIED	19. SECURITY CLASSIFICATION OF ABSTRACT UNCLASSIFIED	20. LIMITATION OF ABSTRACT UL	

INTENTIONALLY LEFT BLANK.

## USER EVALUATION SHEET/CHANGE OF ADDRESS

This Laboratory undertakes a continuing effort to improve the quality of the reports it publishes. Your comments/answers to the items/questions below will aid us in our efforts.

1. ARL Report Number/Author ARL-RP-24 (Joshi) Date of Report June 2001

2. Date Report Received \_\_\_\_\_

3. Does this report satisfy a need? (Comment on purpose, related project, or other area of interest for which the report will be used.) \_\_\_\_\_  
\_\_\_\_\_

4. Specifically, how is the report being used? (Information source, design data, procedure, source of ideas, etc.) \_\_\_\_\_  
\_\_\_\_\_

5. Has the information in this report led to any quantitative savings as far as man-hours or dollars saved, operating costs avoided, or efficiencies achieved, etc? If so, please elaborate. \_\_\_\_\_  
\_\_\_\_\_

6. General Comments. What do you think should be changed to improve future reports? (Indicate changes to organization, technical content, format, etc.) \_\_\_\_\_  
\_\_\_\_\_  
\_\_\_\_\_

CURRENT ADDRESS	_____
	Organization
	Name <span style="float: right;">E-mail Name</span>
	Street or P.O. Box No.
_____	City, State, Zip Code

7. If indicating a Change of Address or Address Correction, please provide the Current or Correct address above and the Old or Incorrect address below.

OLD ADDRESS	_____
	Organization
	Name
	Street or P.O. Box No.
_____	City, State, Zip Code

(Remove this sheet, fold as indicated, tape closed, and mail.)  
**(DO NOT STAPLE)**